Polymer Testing 96 (2021) 107068

Contents lists available at ScienceDirect

Polymer Testing

journal homepage: http://www.elsevier.com/locate/polytest

Study of rheological behaviour of polymer melt in micro injection moulding with a miniaturized parallel plate rheometer

G. Trotta [a,*], B. Stampone [a], I. Fassi [b], L. Tricarico [c]

[a] National Research Council of Italy, Institute STIIMA, Via P. Lembo 38/F, 70124, Bari, Italy
[b] National Research Council of Italy, Institute STIIMA, Via A. Corti 12, 20133, Milano, Italy
[c] Polytechnic of Bari, Mechanical Engineering, Dept. of Mechanics, Mathematics & Management, Via Orabona 4, 70125, Bari, Italy

ARTICLE INFO

Keywords:
Micro injection moulding
Viscosity
Slit flow model
High shear rates
Wall slip
PMMA

ABSTRACT

The study of the rheological behaviour of the polymer in micro cavities is one of the aspects related to the technology of micro injection moulding (μIM) still substantially unresolved. Even today, there are no databases on the rheological characteristics of the material specific for the μIM, which, therefore, takes into account a number of important differences compared to the conventional injection moulding. In this paper, the study of the rheological behaviour of the polymer melt in a thin plate cavity with variable thickness has been conducted. The use of a micro injection moulding machine, on which the prototype of a sensorized mould with pressure and temperature sensor has been mounted, allowed the rheological study of the material under high shear rate conditions. After preliminary tests on different thicknesses, it has been studied the viscosity of polymer melt for 400 μm thickness. The viscosity reduction observed meets the characteristics of a pseudoplastic fluid subject to shear thinning and the wall slip seems to play an important role in the apparent reduction of viscosity. The results suggest to increase injection speed, and consequently injection pressures, so that the reduced viscosity can help melt flow to overcome the extreme conditions due to the aspect ratio and to obtain greater efficiency from the filling phase against the high cooling rate typical of micro injection moulding.

1. Introduction

The increasing interest in micro manufacturing, especially in areas such as aerospace (structure monitoring, sensors for landing system and for engines and reactors, etc.), automotive (pressure sensors, engine management, air and gas quality control, etc …) and above all biomedical, is linked to the results obtained by scientific community that have demonstrated how these micro technologies are ready for the industrial field. In biomedical sector, in particular, the increasing possibility for micro-technologies to be combined in order to produce complete miniaturized devices, are transforming the micro-manufacturing sector in a concrete concept for the factories of the future, where scenarios like the digital twin [1] can be applied to improve the reliability of the process chain. Of all the micro processes, the one that is driving the development towards the mass production in particular of biomedical devices is definitely the micro injection moulding. This technology can be considered a factory in the (micro) factory, because to produce a microfluidic device it is necessary to coordinate several micro-manufacturing technologies in order to obtain the features in the expected range and with high replication capacity [2].

The high cost of micro machining technology to produce cavities for micro injection moulds requires an accurate design of the components supported by a process simulation that need to be as reliable as possible to minimize errors [3]. Current simulation softwares for micro injection moulding process have demonstrated some limitations mainly due to the basic settings that have been defined over time for conventional moulding [4].

Several authors have identified important differences in the definition of the correct HTC (Heat transfer coefficient), which are due to a fast cooling of the polymer melt that is difficult to predict even if it is vital for the correct filling of the component [5,6]. Similarly, it is not yet clear how roughness can affect the filling [7–9] and how this is a further cause of the wall slip [10,11], a melt slip at the interface with the walls of the cavity mould which can result in a viscosity reduction. Moreover, and perhaps more important than the other aspects seen, the rheological

* Corresponding author.
E-mail addresses: gianluca.trotta@stiima.cnr.it (G. Trotta), benedetta.stampone@stiima.cnr.it (B. Stampone), irene.fassi@stiima.cnr.it (I. Fassi), luigi.tricarico@poliba.it (L. Tricarico).

https://doi.org/10.1016/j.polymertesting.2021.107068
Received 17 September 2020; Received in revised form 8 December 2020; Accepted 10 January 2021
Available online 16 January 2021

databases have parameters related to shear rate typical of the standard injection moulding and quite far from the working dynamics of the micro injection moulding [12].

In recent years, commercial rheometers have been developed to study viscosity at high shear rates [13]. They are mainly based on the concept of rotational parallel plate rheometer [14,15] and use rotational velocity to simulate high shear rates [16], unlike a standard capillary or parallel plate rheometer that needs, instead, a piston moved at high speed by a very powerful actuator. The increasing availability of micro injection moulding machines, built with screw or piston systems able to reach injection rates up to 750 mm/s, can become an instrument more similar to the classic rheometers, allowing a viscosity analysis at high shear rates and under real process conditions. This has pushed a small part of the scientific community to build homemade rheometers for micro-moulding to evaluate if and how rheological curves are different compared to the typical curves of conventional moulding.

The common aspect of all prototypes found in literature is that all of them are built using a mould for micro injection to take advantage of the high dynamics of the micro injection moulding machine for experimentation.

The first rheological studies on micro injection moulding date back to 2005 [17] in which a prototype of a square section microchannel rheometer is presented. The square section can vary from 500 μm to 300 μm and 200 μm. Two pressure sensors (Kistler 6159A) have been installed at the inlet and outlet of the microchannel, to measure the difference of pressure and then to calculate the viscosity of the ABS polymer with both capillary model and the slit flow model. The experimentation was carried with mould temperature close to that of the polymer melt, at 200 °C and 210 °C. The results showed, for both temperatures, a tendency of the viscosity curves similar (parallel) to the classical one, but with lower viscosity values, for both models, up to about 50–70% compared to the values obtained with the traditional rheometer for the 200 μm section channel.

The same authors proposed the same approach [17], but with PS (polystyrene) [18] and POM (polyoxymethylene) [19], and for both works a different section of the micro channel, that was reduced to values between 300 μm, 200 μm and 150 μm. For PS, the results confirmed a reduction of viscosity compared to the values obtained with the conventional capillary rheometer, a reduction of viscosity that is directly proportional to the reduction of thickness. For the POM, instead, the results showed a less significant reduction of viscosity compared to PS.

Vasco et al. [20], proposed a rheometer prototype which concept is in line with [17], with two types of microchannel: a rectangular section of 400 μm wide and 100 μm thick, and a square section of 200 μm side. Two pressure sensors (Priamus 6006B) were installed in the same position as seen in Ref. [17]. The capillary model and the slit flow model were used to calculate viscosity based on the measurement of the pressure difference between the two sensors. The material studied was the POM. In order to have a behaviour as close as possible to a capillary rheometer, the filling phase was used without packing to reduce influence on the pressure of interest. The thermal conditions instead, contrary to what seen in Ref. [17], were not isothermal, but they used a mould temperature typical of the real process. The results of the study showed a significant change in the behaviour of the material as shear rate increased for the square section microchannel and this is slightly different from the results obtained in Ref. [18], while there is no clear evidence of the results obtained with the rectangular section microchannel.

In [21] authors used the same approach in Ref. [20] and realized a prototype rheology mould consisting of a microchannel with a variable height from 600 μm to 200 μm with 100 μm pitch. Two pressure/temperature sensors (Kistler 6189A) were conveniently placed before the entry into the microchannel and immediately after the exit from the microchannel; they allow the measurement of the difference in pressure and temperature in the section of interest. The test material is Pebax 7233. The experiment was carried out under non isothermal conditions and considering only the filling phase. The viscosity calculation was performed with the slit flow model considering three melt temperatures, namely 200 °C, 230 °C and 260 °C. The results showed that the viscosity is below the conventional value and, in the range of interest for filling or high shear rate, the slope of the identified curves is greater than the conventional one. Also in this case the results showed a reduced viscosity proportional to reduced thickness.

Mnekbi C. et al. [22] tried to use a capillary rheometer with a variable section from 1 mm to 0,5 mm to increase the shear rate but without success. So to expand the curve to higher shear rates, they used a simulation approach. They simulate the filling in non isothermal condition of a plate of 25 mm × 25 m and 0,5 mm thick. The results confirmed a reduced viscosity compared to the curve with moderate shear rate obtained with the capillary rheometer.

The research activity reported in the paper wants to extend the study on viscosity behaviour of polymer melt at micro level as much as possible to the real process.

The cavity mould geometries proposed in the articles analysed have tried to reproduce as much as possible the geometry of a capillary rheometer inside a mould for micro injection moulding in order to take advantage of the dynamics of micro moulding machines that can reach high speeds, and therefore high shear rate, As shown by proposed literature, these cavity mould geometries fit well with the capillary flow model, less with parallel plates model. Our goal, instead, was to develop a mould for micro rheometry that specifically suites for parallel plates model because it can be more useful to bring rheological models closer to real conditions, such as thin plates for microfluidics applications. In this field of application, it may be very important to analyze the behaviour of the polymer melt in a typical thin cavity to prevent defects that can compromise the functionalities of the device, such as incomplete filling or high shrinkage with conseguent high warpage.

At the purpose, it has been realized a prototype of a mould with the smallest commercial pressure and temperature sensors housed directly in the mould cavity of a typical geometry for micro injection moulding, a thin plate with variable thickness. The geometry proposed in this paper has the aim to increase the complexity of the filling phase thanks to the remarkable aspect ratio of the cross section and the overall size of the cavity. This will amplify the viscous behaviour of the polymer melt so that it can be highlighted in detail the difference between micro and standard injection moulding.

The thicknesses chosen for the study are in line with those reported in the various articles mentioned and specifically related to the micro level, so that it could be possible to compare the results with the state of the art to evaluate similarities and interesting differences observed.

It is also important to underline how the parallel plate rheometer prototype proposed in this work differs in the concept from the versions seen so far. In the adopted solution, the housing of the sensors is realized directly into the real cavity so that it is possible to measure most reliable values without variations due to transition zones, as it happens, instead, for housing solutions seen in literature where the sensors are positioned at the inlet and outlet of the microchannel. This can be a limit, as underlined by Vasco et al. [20] because the sensors read pressure values, and in some cases temperatures, in areas of strong microfluidic transition where pressure and speed can vary considerably due to the sudden variation of the cross-section.

Preliminary designed experiments have been executed with polymethilmethacrylate (PMMA). It is a polymer largely used in the biomedical field due to its biocompatibility, transparency and ability to precisely reproduce microfeatures down to 20 μm when moulded [12]. Rheological studies on capillary rheometer dies with microchannels have been realized [23], but so far from real process conditions as proposed in this paper. Moreover, in line with Vasco et al. [20] and Zhang et al. [21], which have shown that working at different temperatures between mould and polymer does not affect the result, it was considered appropriate to carry out the experimentation under

non-isothermal conditions. The approach allows to evaluate the rheological behaviour as much as possible in operative conditions of production for micro injection moulding.

2. Materials and methods

2.1. Slit flow model

This model is used in parallel plate rheometers. The cavity of a parallel plate rheometer is defined as a rectangular section channel with width w and height h with w ≫ h. The ratio (w/h), between the larger side (width) and the smaller side (height) of the rectangular section, defines the Aspect ratio (AR) used in the article. The effects of pressure drop on edges are negligible. The fused polymer is pushed by a piston into the cavity as shown in Fig. 1.

The assumptions done are of a complete filling of the cavity and a stationary laminar flow of the polymer melted in no slip condition. Viscosity can be calculated by measuring the volume flow rate (Q) of polymer leaving the cavity per unit of time for a given pressure drop (ΔP) as the difference of pressure between consecutive pressure sensors.

In the case of Newtonian fluids in the flow model in parallel plates the apparent shear rate, for which an apparent viscosity can be defined which is linked to the velocity gradient at which it was measured, can be calculated as:

$$\dot{\gamma}_{w(\mathrm{app})} = \frac{6Q}{wh^2} \tag{1}$$

while real shear stress is given by:

$$\tau_{w(real)} = \frac{-\Delta P}{L}\frac{h}{2} \tag{2}$$

where L, indicates the length of the plates as shown in Fig. 1.

It is essential to evaluate the aspect ratio of the rectangular section of the cavity. For Newtonian fluids, shear stress on the wall is [19]:

$$\tau_{w(real)} = \frac{-\Delta P}{L}\frac{wh}{2(w+h)} \tag{3}$$

In the case of non-Newtonian fluids, using Walter's corrections [22] the shear rate at the wall can be calculated as:

$$\dot{\gamma}_{w(\mathrm{app})} = \frac{6Q}{wh^2}\left(\frac{2+\beta}{3}\right) \tag{4}$$

where β is:

$$\beta = \frac{\ln\dot{\gamma}_{w(app)}}{\ln\tau_{w(real)}} \tag{5}$$

For each measurement of $\tau_{(real)}$ and $\gamma_{w(\mathrm{app})}$ it is possible to obtain a point on the real viscosity function by making the correction proposed by Schümmer associated with the representative viscosity model [25] to overcome the difficulty ofβ enhancement. We assume that at the distance y_s the apparent shear rate is equal to the real shear rate; at this point, the stress shear and the apparent shear rate are given by $x^*\tau_w(real)$ and $x^*\gamma_{w(app)}$.

The value of x^* is given by:

$$x^* = \frac{2y_s}{h} \tag{6}$$

The viscosity will, therefore, be given by

$$\eta = \frac{x^*\tau_w}{x^*\dot{\gamma}_{w(app)}} \tag{7}$$

For capillary flows, it can be demonstrated that:

$$x^* = \left(\frac{3\beta+1}{4\beta}\right)^{\frac{\beta}{\beta-1}} \tag{8}$$

and in particular for capillary flows with slit geometry $x^* = 0.79$ [18] and (7) becomes:

$$\eta = \frac{\tau_w}{\dot{\gamma}_{w(app)}} \tag{9}$$

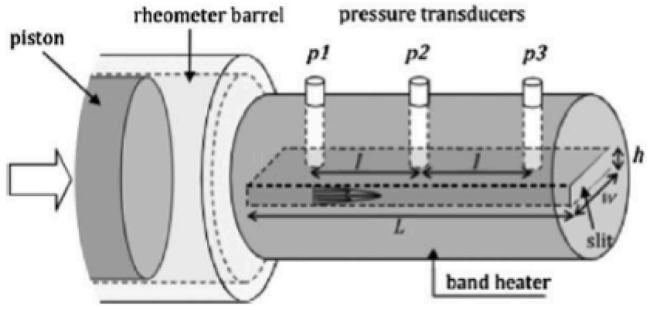

Fig. 1. Scheme of a parallel plate rheometer [20].

2.2. Parallel plate rheometer design

The slit flow rheometer for micro injection moulding viscosity studies on polymers is obtained by the combination of different sub-inserts. As reported in Fig. 2, it is composed of a main mould insert on which it is possible to mount an **end cavity filling insert**, and the **variable height cavity insert** that is the core of the slit flow rheometer. In Fig. 2, it is also possible to see the spacers, which are useful to regulate the desired thickness of the cavity from 700 μm to 100 μm. The combination of spacers of 100 μm thickness with others of 200 μm thickness can guarantee a precise height of the cavity. The sensor housing, on the other hand, was one of the most complex elements both to design and to realize due to the small space in which different components must coexist.

The insert to be able to carry out the rheological tests was assembled inside a master mould (Fig. 3) previously used for the realization of microfluidic components [2] and that has been reused due to its flexibility in terms of reconfigurability with the simple replacement of inserts. From Fig. 3 it is possible to appreciate the complexity of the assembly of both the rheometer insert and the sensors, which are connected externally with a data acquisition system (DAQ).

The basic idea of this project is to study the viscosity of polymers during the filling of a micro injection moulding cavity. The type of component that is obtained from the filling of the cavity proposed is a thin plate (Fig. 4), a type of structure in which the transverse dimension or thickness of the plate is significantly small compared to the length and width dimensions. In this case-study, the thickness is variable between 700 μm and 100 μm with a minimum step of 100 μm.

Different from Chen [17] and Vasco [20], however, the proposed component, and consequently the relative mould cavity, must meet the requirements of a typical parallel plate rheometer, as seen in the previous paragraph in Fig. 1, which means to have a rectangular section with high aspect ratio, as in the case proposed in this paper that is up to 75.

In addition, sensors have been housed near to the gate, after which the flow begins to stabilize, and at the end of the component, where the injection pressure reaches the minimum value. Besides, with sensors positioned in this way, a significant pressure difference was detected even at high injection speeds thanks to a sufficiently large distance between the two sensors.

2.3. Mould insert, machine and material

The inserts have been realized with extremely precise machining techniques (5 axis high precision milling machine) to guarantee

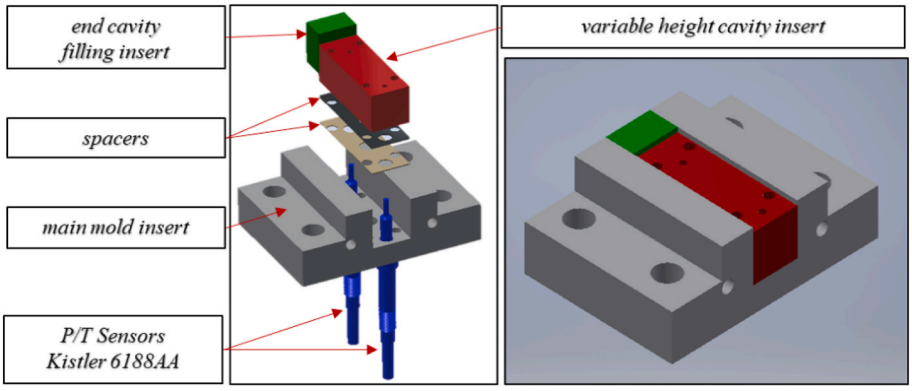

Fig. 2. Explosed and assembled view of the insert for slit flow rheometer.

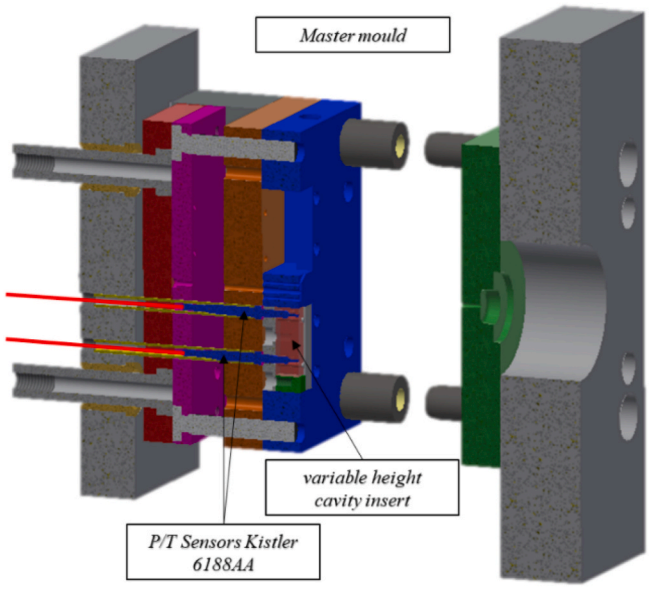

Fig. 3. Overview of the master mould with tool (variable eight cavity insert and sensors) for rheological studies.

micrometric tolerance (Fig. 5a). The top surface of the cavity insert, the one on which the polymer has to slide, has been finished with grinding machine, to guarantee sub-micrometric roughness, together with all surfaces of the master mould that are in contact with the polymer. Micro Electro Discharge Machining (μEDM) technology has been used to realize the precise housing for the sensor on the cavity inserts.

The spacers to vary the cavity height (Fig. 5b), instead, has been realized with femtosecond laser cutting from calibrated stainless steel strips.

The insert has been mounted inside an insert holder plate already used in Ref. [2] (Fig. 6a). Then the P/T sensors have been placed in the insert housings (Fig. 6b) before assembling the whole mould unit.

The complete mould was then mounted on a micro injection moulding machine and the sensors were connected to the acquisition system (DAQ) and from there to the computer on which we created a Labview© data processing software (Fig. 6c).

The experimentation was conducted on a DESMA Tec Formica Plast 1K, a pure micro injection moulding machine, available in our laboratories, equipped with two plungers: a 6 mm diameter plunger for the pre-plasticizing unit and a 3 mm diameter plunger for the injection unit. The machine is characterized by a maximum clamping force of 1 ton, maximum injection pressure that can be regulated up to 3000 bar, maximum injection speed of 500 mm/s and maximum ejection force of

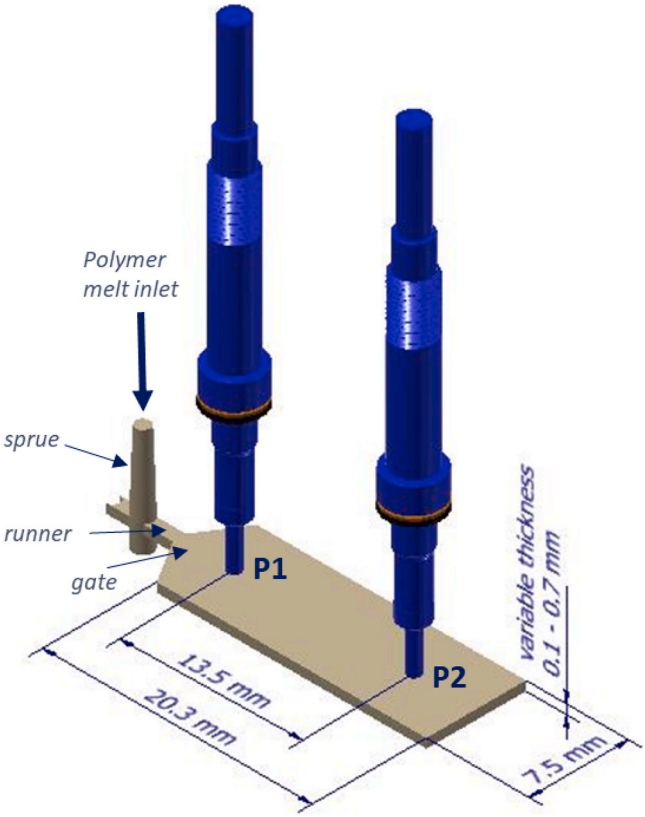

Fig. 4. Layout of the PMMA thin plate with all the cavity parts. (sprue, runner and gate), main dimensions and sensors position.

300 N.

The material used for the experimentation is the ACRYREX® CM-211 by Chi Mei. It is a low viscosity polymethylmethacrylate (PMMA) grade. Exhibits high flowability and easy mould processing. Possesses good cleanliness, high transparency and gloss, stable physical, chemical, optical and electrical properties.

Despite being formed by polymerizing methyl methacrylate (MMA), PMMA is extremely biocompatible. This biocompatibility can be attributed to PMMA's resistance to temperatures stress, chemical reactions, human tissue and bioprocesses. Due to this characteristics it is largely used in biomedical applications.

2.4. Experimental plan to identify best process parameters

Preliminary tests were carried out to verify the feasibility to

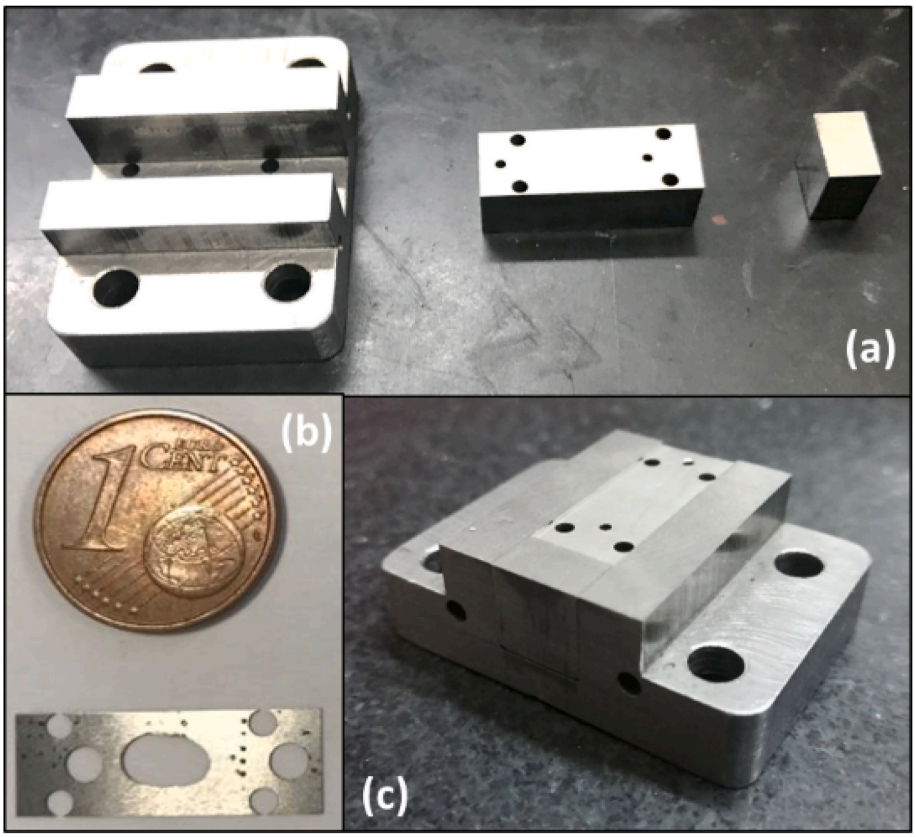

Fig. 5. Mould height cavity variable insert: a) overview of all the parts, b) spacers for cavity height variability and c) final mould insert assembled.

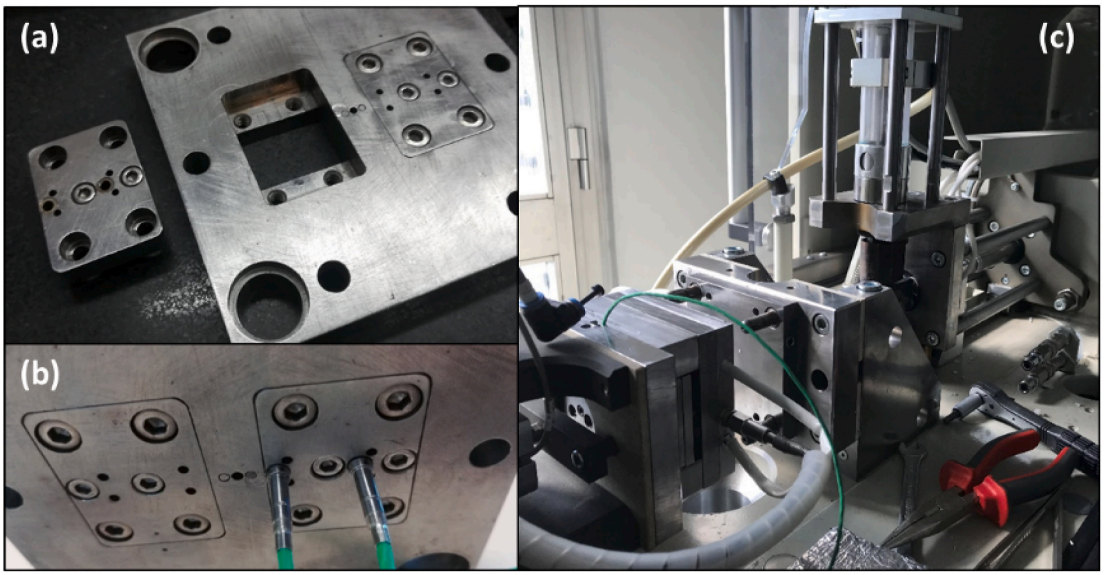

Fig. 6. Overview of the: a) assembly phase of the rheometer insert in the main plate of the master mould; b) sensor installation and c) complete master mould with sensor system mounted on the micro injection moulding machine.

completely fill the equidistant thicknesses of 700, 400 and 100 μm. It was observed, during the tests, that the internal pressures generated during the filling phase increases when increasing injection speed and decreasing cavity thickness. Experimental results have shown a significant influence of the cavity thickness reduction with the tendency to overcome the clamping force, resulting in an increase in injected material compared to what was expected. In particular, the results showed an incomplete filling of 100 μm thickness. Moreover, the partially produced components had a considerable burr probably due to the overcoming, during the injection phase, of the clamping force limit of the machine (Fig. 7). Therefore, the thickness of 100 μm was considered the technological limit of the experimentation, for the type of geometry proposed, and was not subject to further analysis.

An experimental campaign was carried out to identify the best PMMA process parameters for each one of the test pieces of thickness 700 and 400 μm (Fig. 8). A fractional factorial plan replicated 2 times

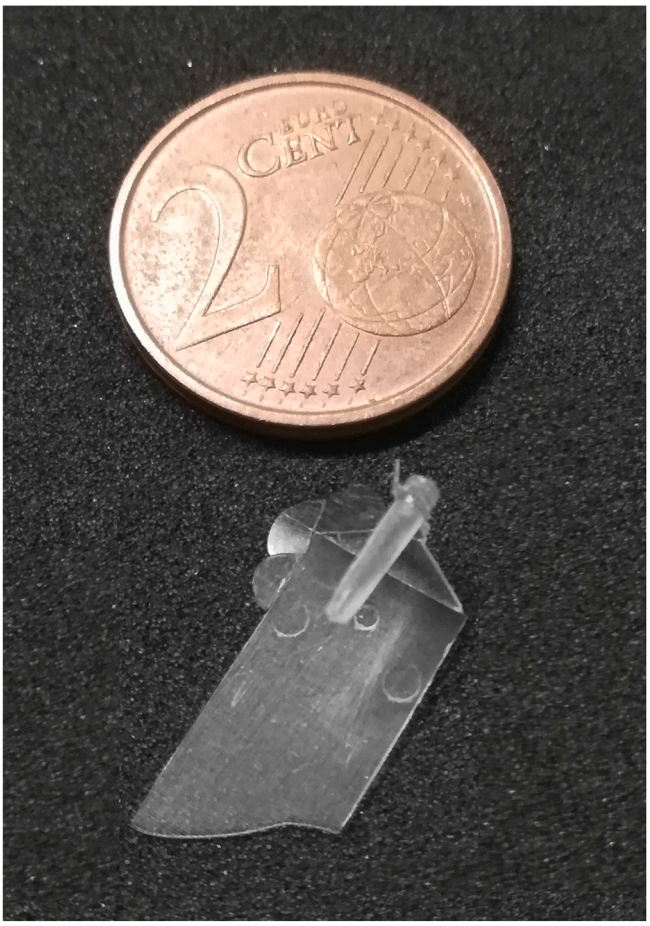

Fig. 7. Example of incomplete filling and burr on test parts in PMMA of 100 μm thickness.

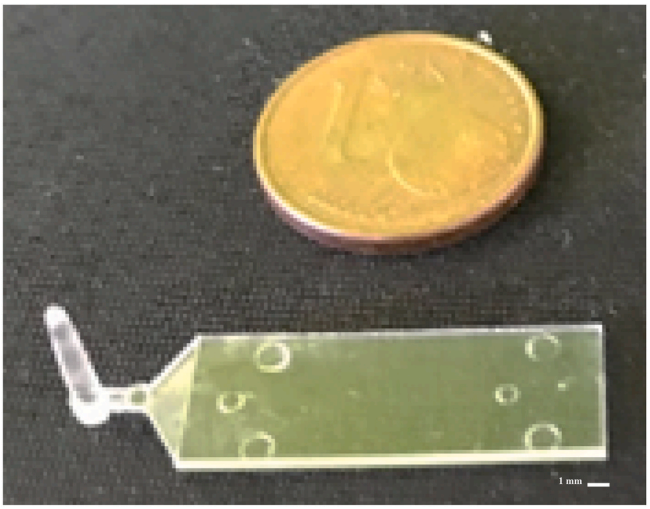

Fig. 8. Example of test part in PMMA (thickness 700 μm).

was set up to minimize the number of experiments. The choice of levels for the factors was made considering the experience done by the authors with this material [2,26].

The process parameters identified for the experimental plan are the ones related to the filling phase:

- Mould temperature (T_{mold})
- Melt temperature (T_{melt});
- Injection speed (v_{inj});
- Maximum injection pressure (Max P_{inj}).

The values of the levels chosen for this fractional factorial plan are shown in Table 1 and the experimental plan is reported in Table 2.

The response variable observed is the pressure difference between the two sensors (ΔP) of eq. (3).

2.5. Experimental plan to built the viscosity curve

For the evaluation of the viscosity curve of the PMMA the attention was focalized on the 400 μm thickness. In order to obtain the pressure values corresponding to high shear rates, it has been considered only the filling phase for the experimentation to avoid any interferences on the cavity pressure due to the packing phase [20].

The filling phase was realized using the short shot approach. It has been set, on the machine, both filling and packing conditions, but in the packing conditions the holding pressure was set at zero. Then, the plunger run, previously set to fill about 99% of the cavity, has been stopped at the switchover position. In this way, according to Vasco et al. [20] and Zhang et al. [21], the process can be preserved from the possible influence of the backpressure due to the complete filling of the component.

Two melt temperatures, namely 230 °C and 250 °C, were defined. A sequence of experimental trials, for each of the melt temperatures, was carried out from 30 mm/s to 270 mm/s with steps of 10 mm/s. For each speed, 15 trials were produced, and the last 10 were used to register the pressure measured by the sensors (Examples of pressure curves for the two sensors in Figs. 9 and 10 respectively for T_{melt} 230 °C and 250 °C).

3. Results and discussion

3.1. Design of experiment analysis

Design of Experiments (DOE) is a useful tool to efficiently determine if key inputs are related to key outputs. Even if DOE is simply a regression analysis, what is not simple, however, is all of the choices you have to make when planning your experiment. Factorial designs assume there is a linear relationship between factors and response variables. Center points can help to evaluate if the relationship between any factor and response variable exhibits linear behaviour or not. They are also useful when added to a replicated plan, to increase the probability of detecting significant factors, and estimate the variability of the process, comparying the pure error, related to the center points, with the real error. This comparison helps to define if the center points can be considered a stable range of process parameters and how this range can be varied to preserve reliable process conditions.

For our experimentation, it has been used n.6 replicates of the center points randomly distributed in the whole factorial plan. For each plan, 10 thin plates have been produced but the last n.5 has been considered for the analysis. The collected data has been analysed with software Minitab19© for both 700 μm and 400 μm thicknesses. In Figs. 11 and 12 are reported the mean value of the n.5 measurements for each center point. This plot is useful to evaluate the variability between the two sensors. In Figs. 13 and 14, instead, are reported all the n.5

Table 1
Process parameters identified for the experimental plan related to the filling phase.

Levels	Process parameters			
	T_{mold} [°C]	T_{melt} [°C]	v_{inj} [mm/s]	Max P_{inj} [bar]
+1	100	260	150	3000
0	80	250	100	2500
−1	60	230	50	2000

Table 2
Fractional factorial plan for each thickness.

Run	T_{mold}	T_{melt}	v_{inj}	Max P_{inj}
1	−1	1	−1	1
2	0	0	0	0
3	1	−1	1	−1
4	0	0	0	0
5	−1	1	1	−1
6	0	0	0	0
7	1	−1	−1	1
8	−1	−1	−1	−1
9	1	1	−1	−1
10	0	0	0	0
11	0	0	0	0
12	−1	−1	1	1
13	1	1	1	1
14	0	0	0	0
15	0	0	0	0
16	0	0	0	0
17	1	−1	−1	1
18	−1	1	−1	1
19	0	0	0	0
20	1	−1	1	−1
21	−1	1	1	−1
22	0	0	0	0
23	0	0	0	0
24	1	1	−1	−1
25	−1	−1	1	1
26	0	0	0	0
27	−1	−1	−1	−1
28	1	1	1	1

measurements done for each center point analysed. This plot is useful to evaluate the variability within the n.5 measurements of the same sensor. The response variable observed is the ΔP of eq. (3).

From Fig. 11 it can be observed that the pressure loss between the first sensor (P1) and the second sensor (P2) is high for both thicknesses, with a difference of pressure ΔP which is about twice for the thickness of 400 μm. It is interesting to observe that the variability of each sensor for both the thicknesses is comparable.

From Fig. 12, instead, it can be observed that the variability within the n.5 measurements for each sensor is comparable too for both thicknesses.

Further study was carried out by comparing the entire experimental plan previously without and then with the center point included for each thickness (Figs. 13 and 14). It can be observed that the center points fit the center values of the measurements done for each sensor and this is a clear evidence of the linear relationship between the factors and the response variable. Observing the distribution of the response variable for both thicknesses and both sensors, it is clear that the variability for the 700 μm thickness (Fig. 13), even if comparable, is greater than that for 400 μm thickness (Fig. 14).

Looking at the pressure measurements of Fig. 14 it is possible to observe that sensor P2 has less variability compared to sensor P1, and this underlines how critical can be the area near to the gate, where cross section geometry changes rapidly. Further analysis highlights that the ΔP for 400 μm thickness is higher than 700 μm thickness, as expected.

The analysis of variance for both thickness 700 μm and 400 showed that for thickness 700 μm (Table 3a), the model can be considered additive, which means that it is composed of only the most significant main factors (with p-value < 0.05). These are B (T_{melt}) and C (v_{inj}) and D (P_{inj}), that have higher value of adj SS (adjusted Sum of Squares that is the amount of variation explained by a term). For the thickness of 400 μm (Table 3b), the model can also be considered additive with C (v_{inj}) as the only value statistically significant (with p-value < 0.05).

Both models have a high R-sq(adj) and this means good reliability of the model identified. What clearly emerges from the comparison of the ANOVA's of Table 3 is that as the thickness decreases, the injection rate of the polymer becomes the factor that best characterizes the pressure variation. This is an aspect that strongly affects the viscosity of the polymer melt due to the inverse proportionality between viscosity and speed (shear rate), as can be deduced from equation (3).

In order not to reject the normal hypothesis, it has been verified that the response variable is distributed normally (Figs. 15a and 16a), that the data are randomly distributed in the sample and that there are no outliers (Figs. 15b and 16b). In addition, Figs. 15b and 16b highlight how standardized residuals fall within the range [+3, −3]. Finally, the hypothesis of homogeneity of variance (homoscedasticity) cannot be rejected, as can be seen from the result of the Bartlett test for normal distribution (Figs. 15c and 16c).

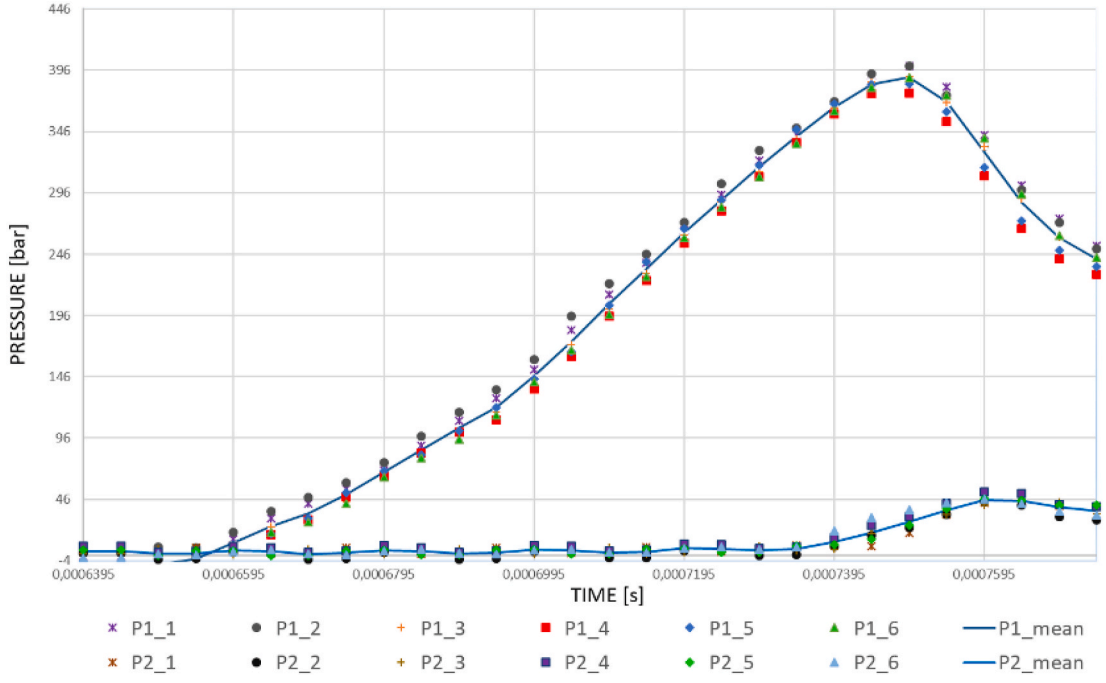

Fig. 9. Example of pressure curves obtained from sensors P1 and P2 at T_{melt} = 230 °C - thickness 400 μm.

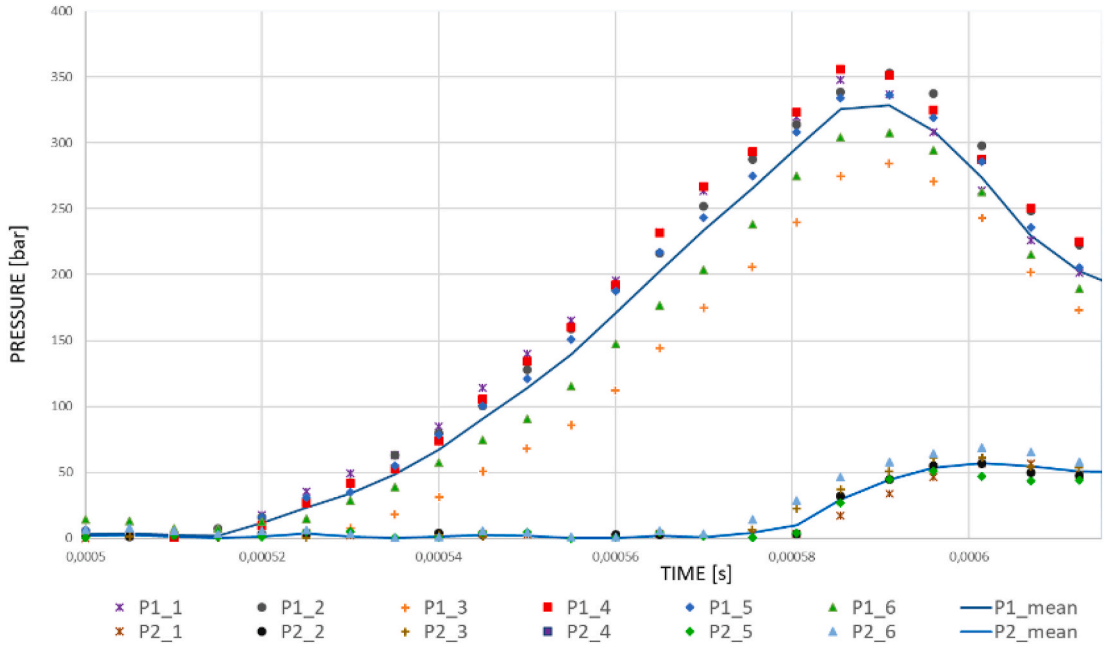

Fig. 10. Example of pressure curves obtained from sensors P1 and P2 at Tmelt = 250°C- thickness 400 μm.

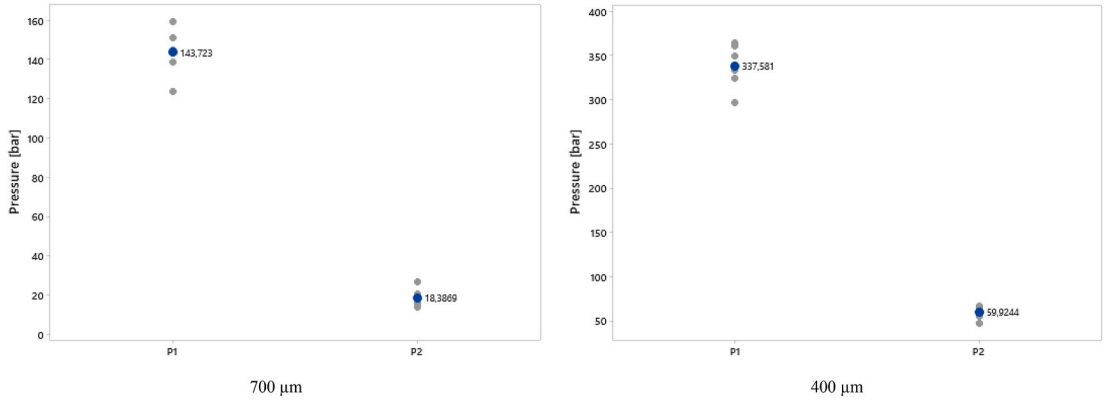

Fig. 11. Individual value plot of center points for P1 and P2 averaged over n.5 measurements - thickness 700 μm and 400 μm.

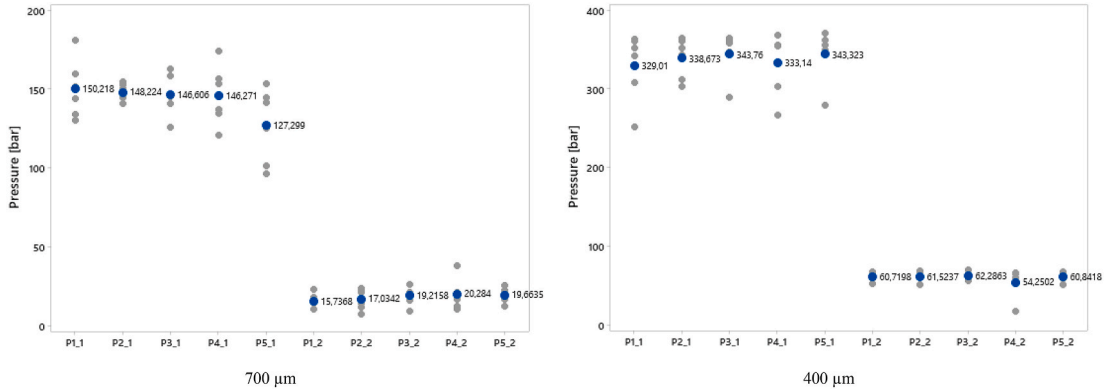

Fig. 12. Pressure values of replicas of center point for P1 and P2 - thickness 700 μm and 400 μm.

3.2. Viscosity curves at a high shear rate

The experimental results obtained using the proposed parallel plate rheometer with a thickness of 400 μm were used for the analysis of the viscosity in the micro injection moulding. Compared to the results obtained with the other plate thicknesses investigated and based on literature results, this thickness can be considered close to the limit of the technological feasibility of the process for this type of component. The

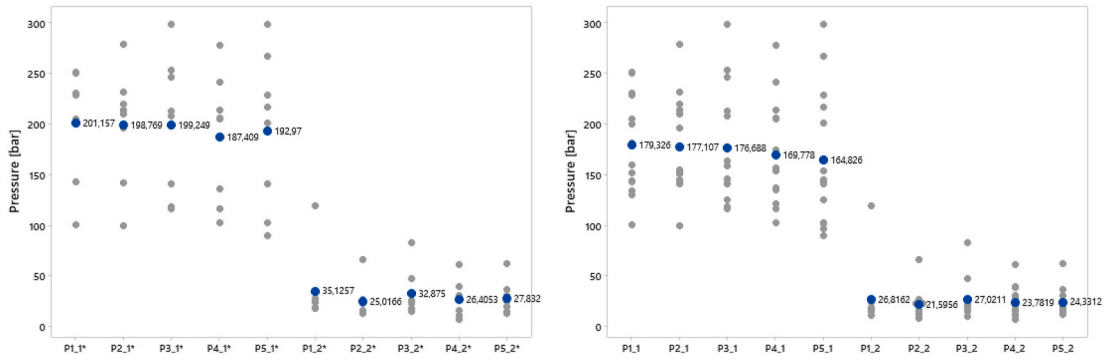

Fig. 13. DoE plan without and with center point for P1 and P2. - 700 μm thickness.

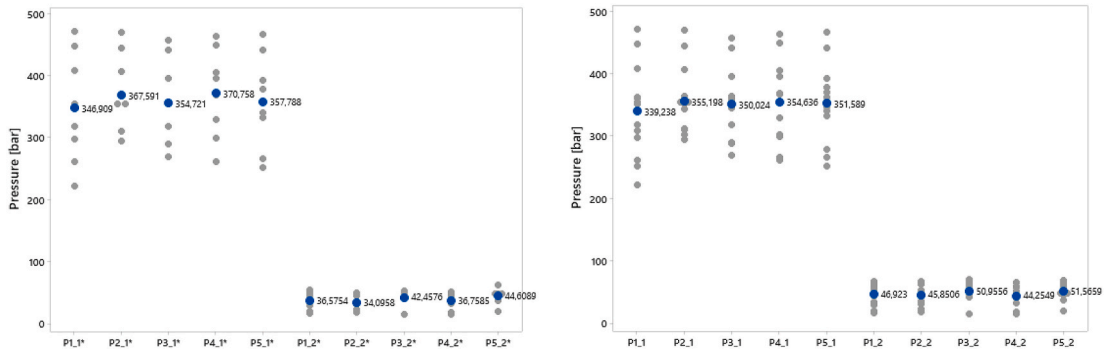

Fig. 14. DoE plan without and with center point for P1 and P2 400 μm thickness.

Table 3
Analysis of variance (ANOVA) – Difference of Pressure between P1 and P2 (ΔP).

(a) Thickness 700 μm						(b) Thickness 400 μm					
Source	DF	Adj SS	Adj MS	F-Value	P-Value	Source	DF	Adj SS	Adj MS	F-Value	P-Value
Model	9	182235	20248	33,39	0,000	Model	9	656597	72955	54,58	0,000
Blocks	1	155064	155064	255,73	0,000	Blocks	1	639387	639387	478,36	0,000
Linear	4	18230	4558	7,52	0,001	Linear	4	12834	3209	2,40	0,088
A	1	145	145	0,24	0,631	A	1	242	242	0,18	0,675
B	**1**	**8842**	**8842**	**14,58**	**0,001**	B	1	1154	1154	0,86	0,365
C	**1**	**6538**	**6538**	**10,78**	**0,004**	**C**	**1**	**11236**	**11236**	**8,41**	**0,010**
D	**1**	**2705**	**2705**	**4,46**	**0,049**	D	1	202	202	0,15	0,702
2-Way Interactions	3	2082	694	1,14	0,358	2-Way Interactions	3	4375	1458	1,09	0,378
A*B	1	1850	1850	3,05	0,098	A*B	1	23	23	0,02	0,897
A*C	1	232	232	0,38	0,544	A*C	1	46	46	0,03	0,855
A*D	1	1	1	0,00	0,969	A*D	1	4306	4306	3,22	0,089
Curvature	1	6858	6858	11,31	0,003	Curvature	1	2	2	0,00	0,973
Error	18	10915	606			Error	18	24059	1337		
Lack-of-Fit	8	10079	1260	15,07	0,000	Lack-of-Fit	8	20592	2574	7,42	0,002
Pure Error	10	836	84			Pure Error	10	3468	347		
Total	27	193150				Total	27	680657			
Reliability of the model						**Reliability of the model**					
S		R-sq	R-sq(adj)	R-sq(pred)		S		R-sq	R-sq(adj)	R-sq(pred)	
24,6245		94,35%	**91,52%**	78,11%		36,5600		96,47%	**94,70%**	86,20%	

slit flow rheological model and in particular, the equations in section 2.1 were used to design the viscosity curves, starting from the ΔP and time as variables available at the end of the experimentation. Even if the slit flow model does not take into account the effect of temperature, data acquired by the two temperature sensors allowed to support result analysis. In addition, these data are useful for subsequent implementation of temperature-dependent models, such as that of Cross- WLF.

Figs. 17 and 18 show the viscosity curves obtained from the experiments respectively at 230 °C and 250 °C; for comparison, the same figures highlight the viscosity curves measured with standard rheometers (standard viscosity curves from online Campus® database and compared with Moldflow© database) for the PMMA used in the experiments. The area of interest is the one evidenced with a coloured square (red one for viscosity at T_{melt} 250 °C and green one for viscosity at T_{melt} 230 °C) that corresponds to high shear rates (from 10∧3 to 10∧6 s^{-1}). In the same section, even the experimental curves can be fitted with a linear model, according to the high R2 obtained (Figs. 17 and 18), but with a greater slope respect to that of the standard viscosity curve, for both melt temperatures investigated. This means that for micro injection moulding it is necessary to set high injection speed, and consequently high injection pressures in order to reduce viscosity to overcome the extreme conditions due to the aspect ratio. In this way, it is possible to

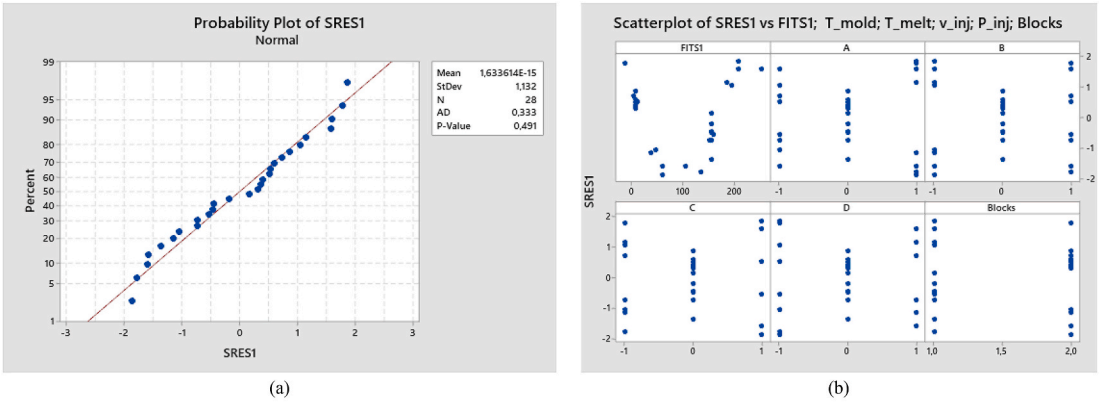

(a) (b)

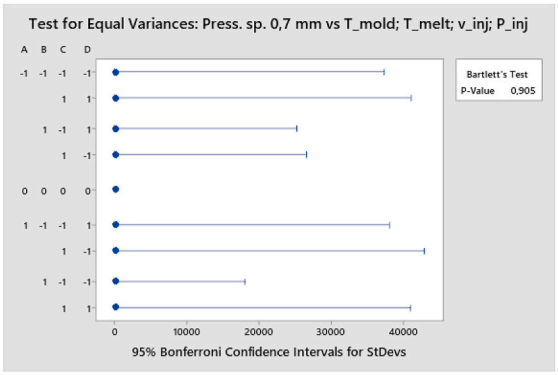

(c)

Fig. 15. – Thickness 700 μm - a) normality test; b) outliers analysis; c) Test of equal variance.

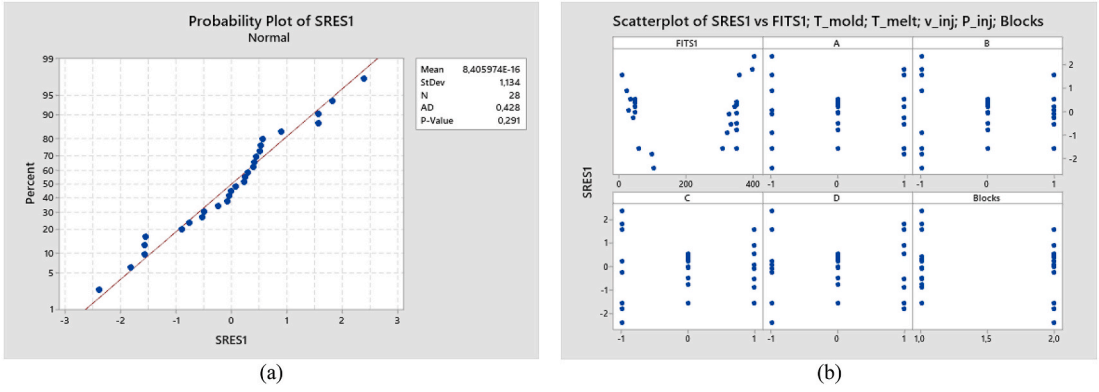

(a) (b)

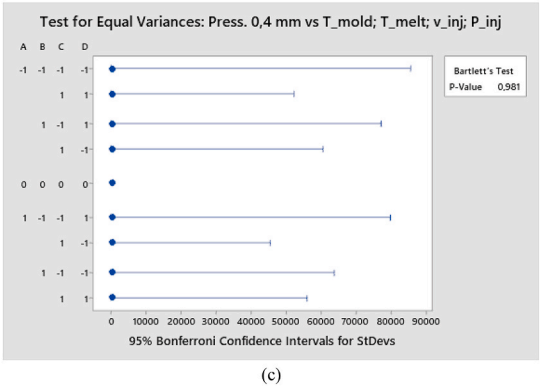

(c)

Fig. 16. Thickness 400 μm - a) normality test; b) outliers analysis; c) Test of equal variance.

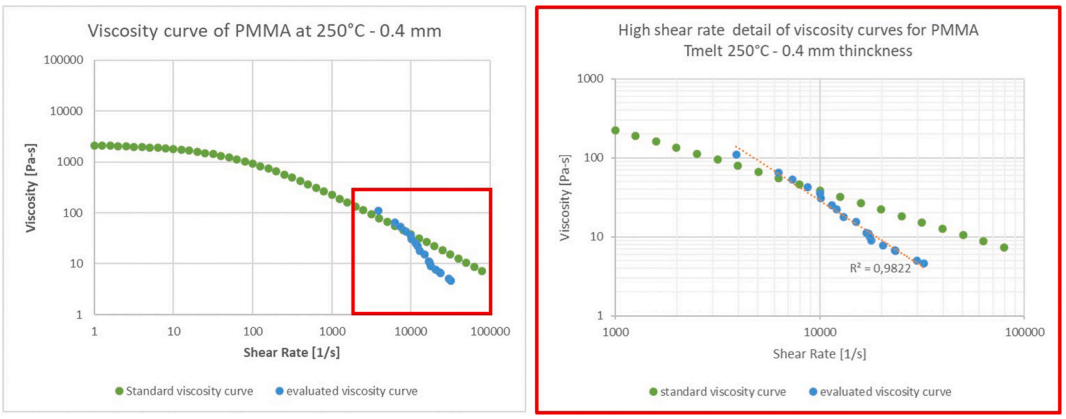

Fig. 17. Comparison between the standard viscosity curve and the one obtained by experimentation for PMMA at Tmelt = 250 °C Vinj 30 ÷ 270 mm/s (step 10 mm/s) – thickness 400 μm.

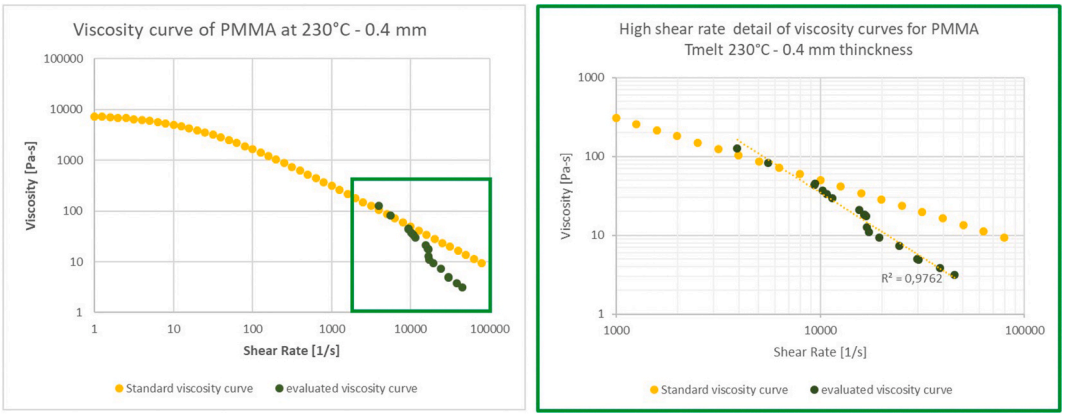

Fig. 18. Comparison between the standard viscosity curve and the one obtained by experimentation for PMMA at T_{melt} = 230 °C V_{inj} 30 ÷ 270 mm/s (step 10 mm/s) – thickness 400 μm.

obtain higher efficient filling phase able to fill the whole cavity against the high cooling rate.

The viscosity reduction observed (Figs. 16 and 17) is in line with the results available in literature for micro injection moulding [21] and meets the characteristics of a pseudoplastic fluid subject to shear thinning, as discussed in detail in the analysis proposed below.

One of the most widely used forms of the general non-Newtonian constitutive relation is a power-law model, which can be described, as introduced by Bird et al. [27]:

$$\tau = m\dot{\gamma}^n \tag{10}$$

Where τ is shear stress, $\dot{\gamma}$ is shear rate and m, n are power-law model constants. The constant m is a measure of the consistency of the fluid: the higher the value of m, the more viscous the fluid is. The exponent n is a measure of the degree of non-Newtonian behaviour: the greater the departure from the unity, the more pronounced the non-Newtonian properties of the fluid are. Viscosity for the power-law fluid can be expressed as:

$$\eta = m\dot{\gamma}^{n-1} \tag{11}$$

where η is the non-Newtonian apparent viscosity. If $n < 1$, as it is the case of the proposed paper, a shear thinning fluid is obtained; a progressively decreasing apparent viscosity with an increasing shear rate [26] characterizes such a fluid.

Shear thinning is the non-Newtonian behaviour of fluids whose viscosity decreases under shear strain. It is sometimes considered synonymous for pseudoplastic behaviour. Though the exact cause of shear thinning is not fully understood, it is widely regarded to be the effect of small structural changes within the fluid, such that microscale geometries within the fluid rearrange to facilitate shearing. In melted polymers, shear thinning is caused by the disentanglement of polymer chains during flow. At rest, high molecular weight polymers are entangled and randomly oriented. However, when sheared at a high enough rate, these highly anisotropic polymer chains start to disentangle and align along the direction of shear. This leads to less molecular/particle interaction and a larger amount of free space, decreasing the viscosity.

As reported in literature, other effects could play a role in the reduction of viscosity in micro injection moulding, such as viscous dissipation, polymer compressibility and wall slip. All these effects are "surface effects" strictly related to the roughness of the cavity mould and consequently to the melt flow temperature at the interface with the cavity mould.

In Fig. 19 is reported the comparison between temperatures measured with the two sensors at different injection speeds and at T_{melt} of 250 °C. The temperatures read by the sensors are related to the layer directly in contact with the mould cavity, so in the area of interest to observe surface effects on viscosity. The reduced temperature observed is a clear evidence of the high cooling rate in micro injection moulding. The temperature variation (ΔT) between the two sensors is quite small and tends to decrease according to the injection rate.

Analysing in detail the literature related to the cavity surface effects for the same aspect ratio, and considering the temperature results of Fig. 19 and the cavity insert roughness (section 2.3), other effects do not significantly influence the viscosity results obtained and the slit flow model is sufficiently representative of the melt behaviour for this type of

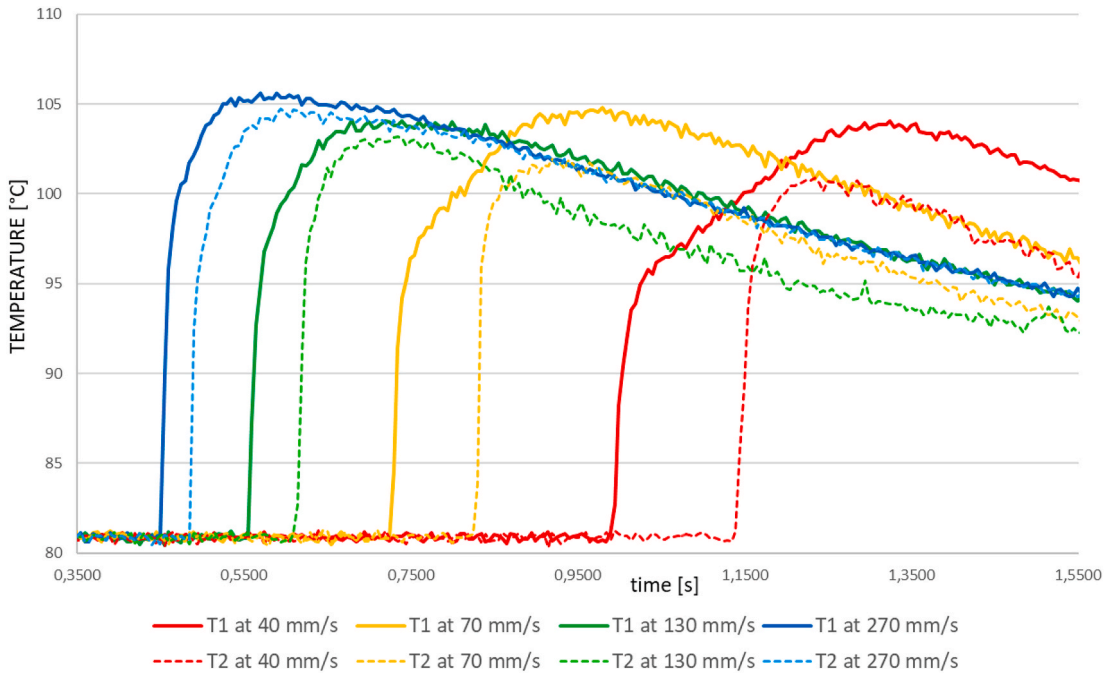

Fig. 19. Example of comparison between temperature measurements for sensor 1 (T1) and sensor 2 (T2) at different injection speeds (v_{inj}) and for T_{melt} of 250 °C.

cavity.

Viscous dissipation is an effect due to the viscous friction that is generated between the molten polymer and the surface (roughness). The effect is obviously an increase in the temperature of the molten polymer that could consequently affect the viscosity contributing to its reduction. The contribution of viscous dissipation to the rise in temperature is therefore essentially due to the roughness of the mould cavity. However, the incidence in the micro field has been the subject of studies mainly by Bin Xu et al. [28] which, from a study conducted on microchannels of 1000 μm, 500 μm and 350 μm thickness, deduced that viscous dissipation does not play an important role in microcavities. The same authors observe that the temperature of the polymer in contact with the mould cavity tends to grow due to the high shear rate, while the temperature remains substantially unchanged at the center of the microcavity because of the reduced influence of roughness. The variation of local viscosity is probably small compared to the general viscosity evaluated and the viscous dissipation effect can be neglected if the cavity has been worked with a low roughness, as for the work presented (section 2.3).

In order to verify what has been stated in the cited paper, the Eckert number and the Brinkman number have been evaluated. These dimensionless number are essential to evaluate heat conduction between a wall and a flowing viscous fluid. The Eckert number (E_c) is a dimensionless quantity useful in determining the relative importance in a heat transfer situation of the kinetic energy of a flow. It is the ratio of the kinetic energy to the enthalpy (or the dynamic temperature to the temperature) driving force for heat transfer:

$$E_c = \frac{U^2}{c_p \Delta T} \tag{12}$$

where U is the fluid velocity, c_p is the specific heat at constant pressure and ΔT is the difference between melt and wall temperature and can be considered the heat dissipation potential.

For small Eckert number (Ec ≪ 1) the terms in the energy equation (12) describing the effects of pressure changes, viscous dissipation, and body forces on the energy balance can be neglected and the equation reduces to a balance between conduction and convection.

According to the real case presented in the paper, the ΔT is quite high because we compare the temperature of the melt (250 °C and 230 °C) with the temperature at the wall (80 °C). According to this observation, the Eckert number (Ec) is surely less than 1 (in the high shear rate range examined we have an Ec number between 3*10∧-4 and 2*10∧-2) and the contribution of viscous dissipation is reduced.

The Eckert number, when multiplied by the Prandtl number (Pr), becomes a dimensionless number related to heat conduction from a wall to a flowing viscous fluid and is usually identified as Brinkman number (Br).

$$Br = Pr^* E_c = \frac{U^2 \eta}{\lambda(\Delta T)} \tag{13}$$

where η and λ (0,19 $[W/m^\circ C]$for PMMA) are the dynamic viscosity and the conductivity, respectively, of the fluid. Considering equation (1) we can have that:

$$u = \frac{\dot{\gamma}_{w(app)}\, h}{6} \tag{14}$$

The Brinkman number (Br) is essentially the ratio between heat produced by viscous dissipation and heat transported by molecular conduction. The higher its value, the slower the conduction of heat produced by viscous dissipation and hence the larger the temperature rise. When (Br) ≪ 1, the energy dissipation can be neglected relative to heat conduction in the fluid. So, the considerations done for the Eckert number can be applied also to the Brinkman number (the Brinkman number, for the range of high shear rates examined in this paper, is between 0.23 and 0.67, in line with the results observed in Ref. [21], and its effect on viscosity reduction can be considered less influential).

The compressibility of the molten polymer has important effects on pressure and density distribution in the filled part and the effect of melt compressibility becomes more pronounced with a decrease in part thickness [29]. In particular, the numerical investigation indicates that surface roughness and compressibility of the melt influence the flow front, cavity pressure, part density as well as part shrinkage [30]. Analysing in detail the cited papers, the polymer melt compressibility is strongly linked to the variation of local density that contributes to a thickness reduction of part with consequent increase of the inner pressure. However, the authors have pointed out that the temperature, instead, tends to decrease slightly especially for the thickness of 370 μm.

The authors linked this behaviour to the presence of roughness that, in the case of micro moulding and cavities with high aspect ratio, would tend to increase the effect of heat transfer coefficient (HTC) and then heat dissipation. So, the compressibility of thin plates has no direct effect on speed and above all plays no significant role on the viscosity of the component and therefore can be neglected for the experimental analysis that has been carried out.

Wall slip is the term used when fluids violate the classic no-slip boundary conditions of Newtonian fluid mechanics, and do actually slip over solid surfaces when the shear stress exceeds a critical value, as it happens in the micro injection moulding. Zhang et al. [21] described the behaviour of the polymer at different thicknesses by analysing in detail also the work of Vasco et al. [20]. The authors highlighted how the relative slip velocity decreases with increasing thickness and have also noted that it can be identified a strong slip regime at high shear stresses. Comparying Figs. 16 and 17 with the viscosity curve of [21] we can notice an equivalent polimer melt behaviour at high shear rates. So, the slope of the curves is higher than the one expected for non-Newtonian fluids. In fact in standard conditions the shear stress increase while increasing shear rates. In our case, as Zhang et al. [21] highlighted in their paper, polymer melts might be located in the strong stick-slip regime and disentanglement of polymer chains, due to shear thinning, induces stress relaxation. This behaviour is evident in Fig. 20, where, for high shear rates (between 10,000 and 100,000 evidenced with red circle) and T_{melt} of 250 °C, the shear stress is growing slower than standard conditions, and this highlights how wall slip effect is strictly related to reduction of viscosity at high shear rates in micro injection moulding.

It is well known that the temperature increase is the cause of viscosity reduction, but at the same time it is known that a critical shear rate can be the cause of a slip of the material in contact with cavity wall resulting in apparent reduction of viscosity. If we focus on the above viscous dissipation analysis, the results of dimensionless numbers tell us that the contribution of viscous dissipation is less influential on viscosity and therefore the reduction of viscosity cannot be considered a direct consequence of an increase of temperature due to viscous dissipation. Surely the reduced surface friction, due to the low surface roughness, has contributed to the reduction of the effect of this surface phenomenon on viscosity. However, the viscosity results obtained (Figs. 17 and 18) are below the prediction curves of the Carreau-Yasuda model, which is a model under no-slip conditions. This means that the wall slip plays a fundamental role in the reduction of viscosity and that its influence is proportional to the surface roughness, as evidenced by Zhang et al. [21]. This aspect, however, requires a more in-depth investigation with the help of a numerical approach with which, by exploiting the obtained viscosity models, it is possible to better detail the observed phenomena and their influence on viscosity.

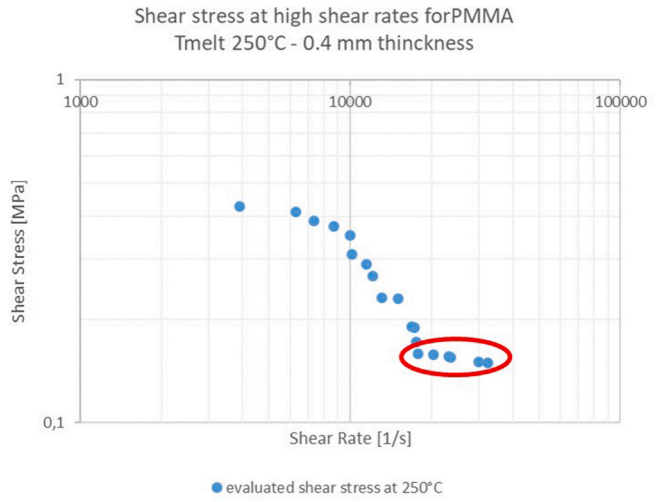

Fig. 20. High shear rates induce a relaxation of shear stress (red circle) due to shear thinning conditions. (For interpretation of the references to colour in this figure legend, the reader is referred to the Web version of this article.)

4. Conclusions

In the present paper, the viscosity curves at different melt temperatures, namely 230 °C and 250 °C for micro injection moulding have been presented.

They have been obtained, for cavity thickness of 400 μm, varying the injection speed from 30 mm/s up to 270 mm/s with steps of 10 mm/s in order to obtain the value of pressure at high shear rate (from 10∧3 to 10∧6 1/s).

A parallel plate rheometer mould with variable cavity thickness has been designed and realized for the rheological studies with slit flow model.

The results obtained show a reduced viscosity at high shear rates and suggest to increase injection speed, and consequently injection pressures, so that the reduced viscosity can help melt flow to overcome the extreme conditions due to the aspect ratio and to obtain greater efficiency from the filling phase against the high cooling rate typical of micro injection moulding.

In order to evaluate the robustness of the viscosity results obtained, a supplementary analysis of the surface effects, such as viscosity dissipation, polymer compressibility and wall slip, has been done taking under consideration also the temperature measurements obtained with cavity sensors and the low roughness of the surface insert.

The viscosity reduction observed (Figs. 17 and 18) meets the characteristics of a pseudoplastic fluid subject to shear thinning and the analysis of the possible surface effects that could participate in the viscosity reduction at high shear rates evidenced a less influential impact of viscous dissipation and compressiblity effects on the viscosity results obtained for the thickness observed, while the wall slip seems to play an important role in the apparent reduction of viscosity.

These results, however, require an in-depth analysis with the help of a numerical approach, so that the viscosity model obtained could be used to calibrate the simulator in order to better detail the influence that shear thinning and wall slip have on viscosity behaviour of the polymer melt for micro injection moulding process.

5. Future developments

Future studies will focus on the thickness window from 400 up to 100 μm to better understand the viscosity behaviour of the polymer melt for higher aspect ratios. For the purpose numerical approach will be used, together with experimentation, to implement a complex viscosity model, such as Cross-WLF, that takes into account also the contribution of the temperature.

Funding

This research work has been done under the framework of the project EXTREME (innovative technologies for EXTREMely Efficient spark ignited engines) of the Axis II - PON Research and innovation 2014–2020 supported by the Ministry of Research and Univeristy – code ARS01_00849 - decree n. 271 of March 04, 2020.

Author statement

The proposed revisions has been positively received by the authors and each suggestion found an appropriate integration in the text. Reviewer observations have concretely helped to improve the overall quality of the paper and have been further analysed and discussed in the Rebuttal Letter to Reviewers.

The authors believe that the article, in its current configuration and after this further improvement effort, has answered to all the required

editing needs and is ready for publication.

Declaration of competing interest

The authors declare that they have no known competing financial interests or personal relationships that could have appeared to influence the work reported in this paper.

Acknowledgments

The authors would like to thank both Annalisa Volpe and Antonio Ancona of CNR IFN for their support with femtosecond laser, Francesco Modica of STIIMA CNR for his support with micro electro discharge machining (μEDM) and Vito Basile of STIIMA CNR for his support with sensors data acquisition system.

Appendix A. Supplementary data

Supplementary data to this article can be found online at https://doi.org/10.1016/j.polymertesting.2021.107068.

References

[1] G.E. Modoni, M. Sacco, W. Terkaj, A telemetry-driven approach to simulate data-intensive manufacturing processes, Procedia CIRP 57 (2016) 281–285, https://doi.org/10.1016/j.procir.2016.11.049.
[2] G. Trotta, R. Martínez Vázquez, A. Volpe, F. Modica, A. Ancona, I. Fassi, R. Osellame, Disposable optical stretcher fabricated by microinjection moulding, Micromachines 9 (2018) 388.
[3] H. Zhang, F. Fang, M.D. Gilchrist, N. Zhang, Precision replication of micro features using micro injection moulding: process simulation and validation, Mater. Des. 177 (2019) 107829.
[4] Can Yang, Xiao-Hong Yin, Guang-Ming Cheng, Microinjection molding of microsystem components: new aspects in improving performance, J. Micromech. Microeng. 23 (2013), https://doi.org/10.1088/0960-1317/23/9/093001, 093001.
[5] T. Nguyen-Chung, G. Jüttner, C. Löser, T. Pham, M. Gehde, Determination of the heat transfer coefficient from short-shots studies and precise simulation of microinjection molding, Polym. Eng. Sci. 50 (1) (2010) 165–173.
[6] Y. Liu, M. Gehde, Evaluation of heat transfer coefficient between polymer and cavity wall for improving cooling and crystallinity results in injection molding simulation, Appl. Therm. Eng. 80 (2015) 238–246.
[7] H.L. Zhang, N.S. Ong, Y.C. Lam, Effects of surface roughness on microinjection molding, journal of Plymer Engineering and Science 47 (12) (2007) 2012–2019, https://doi.org/10.1002/pen.20904.
[8] R. Surace, M. Sorgato, V. Bellantone, F. Modica, G. Lucchetta, I. Fassi, Effect of cavity surface roughness and wettability on the filling flow in micro injection molding, J. Manuf. Process. 43 (2019) 105–111, https://doi.org/10.1016/j.jmapro.2019.04.032.
[9] L. Wang, Q. Li, W. Zhu, et al., Scale effect on filling stage in micro-injection molding for thin slit cavities, Microsyst. Technol. 18 (2012) 2085–2091, https://doi.org/10.1007/s00542-012-1545-6.
[10] N.S. Ong, H.L. Zhang, Y.C. Lam, Three-dimensional modeling of roughness effects on microthickness filling in injection mold cavity, Int. J. Adv. Manuf. Technol. 45 (2009) 481, https://doi.org/10.1007/s00170-09-1984-0.
[11] Y. Lou, C. Bai, J.-L. Pei, P.-Q. He, A novel micro wall slip model based on chain length and temperature, Int. Polym. Process. 31 (2) (2016) 239–246.
[12] U.M. Attia, S. Marson, J.R. Alcock, Micro-injection moulding of polymer microfluidic devices, Microfluid. Nanofluidics 7 (2009) 1, https://doi.org/10.1007/s10404-009-0421-x.
[13] D. Tang, F.H. Marchesini, L. Cardon, D.R. D'hooge, Evaluating the exit pressure method for measurements of normal stress difference at high shear rates, J. Rheol. 64 (2020) 739, https://doi.org/10.1122/1.5145255.
[14] C.J. Pipe, T.S. Majmudar, G.H. McKinley, High shear rate viscometry, Rheol. Acta 47 (2008) 621–642, https://doi.org/10.1007/s00397-008-0268-1.
[15] Malvern Panalytical, Using a rotational rheometer for high shear rate measurements. https://www.materials-talks.com/blog/2016/04/12/using-a-rotational-rheometer-for-high-shear-rate-measurements/, 2016.
[16] O. Kravchuk, J.R. Stokes, Review of algorithms for estimating the gap error correction in narrow gap parallel plate rheology, J. Rheol. 57 (2013) 365, https://doi.org/10.1122/1.4774323.
[17] S.C. Chen, R.I. Tsai, R.D. Chien, T.K. Lin, Preliminary study of polymer melt rheological behavior flowing through micro-channels, Int. Commun. Heat Mass Tran. 32 (3–4) (2005) 501–510, https://doi.org/10.1016/j.icheatmasstransfer.2004.07.004.
[18] R.D. Chien, W.R. Jong, S.C. Chen, Study on rheological behavior of polymer melt flowing through micro-channels considering the wall-slip effect, J. Micromech. Microeng. 15 (2005) 18, https://doi.org/10.1088/0960-1317/15/8/003.
[19] Chun-Sheng Chen, Shia-Chung Chen, Wei-Lianq Liaw, Rean-Der Chien, Rheological behavior of POM polymer melt flowing through micro-channels, Eur. Polym. J. 44 (6) (2008) 1891–1898, https://doi.org/10.1016/j.eurpolymj.2008.03.007.
[20] J.C. Vasco, J.M. Maia, A.S. Pouzada, Thermo-rheological behaviour of polymer melts in microinjection moulding, J. Micromech. Microeng. 19 (2009) 10, https://doi.org/10.1088/0960-1317/19/10/105012.
[21] N. Zhang, M.D. Gilchrist, Characterization of thermo-rheological behavior of polymer melts during the micro injection moulding process, Polym. Test. 31 (6) (2012) 748–758, https://doi.org/10.1016/j.polymertesting.2012.04.012.
[22] C. Mnekbi, M. Vincent, J.F. Agassant, Polymer rheology at high shear rate for microinjection moulding, Int. J. Material Form. 3 (2010) 539–542, https://doi.org/10.1007/s12289-010-0826-9.
[23] B. Xu, Y.B. Lu, G.M. Li, S. Xue, B.P. Xiang, Rheological behavior of polymethyl methacrylate (PMMA) filling through micro channels, Adv. Mater. Res. 189–193 (2011) 451–454. https://doi.org/10.4028/www.scientific.net/amr.189-193.451.
[25] J.M. Dealy, J. Wang, Melt Rheology and its Applications in the Plastics Industry, vol. XVI, Springer Book ed. Engineering Materials and Processes, 2013, p. 282, https://doi.org/10.1007/978-94-007-6395-1.
[26] G. Trotta, A. Volpe, A. Ancona, I. Fassi, Flexible micro manufacturing platform for the fabrication of PMMA microfluidic devices, J. Manuf. Process. 35 (2018) 107–117, https://doi.org/10.1016/j.jmapro.2018.07.030.
[27] R.B. Bird, C.F. Curtiss, C. Armstrong, O. Hassager, Dynamics of Polymeric Liquids, Volume 2: Kinetic Theory, second ed., Wiley, 1987, ISBN 978-0-471-80244-0, 487.
[28] B. Xu, M. Wang, T. Yu, et al., Viscous dissipation influencing viscosity of polymer melt in micro channels, J. Mech. Sci. Technol. 24 (2010) 1417–1423, https://doi.org/10.1007/s12206-010-0420-6.
[29] Q.M.P. Nguyen, X. Chen, Y.C. Lam, C.Y. Yue, Effects of polymer melt compressibility on mold filling in micro-injection molding, J. Micromech. Microeng. 21 (2011) 9.
[30] Q.M.P. Nguyen, X. Chen, Y.C. Lam, C.Y. Yue, Effect of mold surface roughness on compressible flow of micro-injection molding, International Journal of Industrial and Manufacturing Engineering 6 (2012) 5.

Gianluca Trotta. MSc degree in Mechanical Engineering (2003) from Polytechnic of Bari, Italy. Since 2009, he is full-time researcher at CNR-STIIMA, and as part of MEDIS Group, his research activity focuses on micro manufacturing and in particular on the design and manufacturing of micro devices and micro components with micro-injection moulding. He has been involved in various National and European projects. He is reviewer of international journals and conferences and authors of several scientific papers on international journals, book chapters and conference proceedings. From 2004 to 2009 he worked as industrial researcher for PRIMA Industrie S.p.a. in the R&D area as Laser Technology and Applications Specialist and later as Responsible of the Fiber Laser Technology Laboratory.

Benedetta Stampone. MSc degree in mechanical Engineer (2019) from Polytechnic of Bari. Actually, she is a research fellow at STIIMA CNR and her research activity is focused on modeling and optimization of the micro injection moulding process.

Irene Fassi. PhD (2001), MSc in Mechanical Engineering (1997) from Polytechnic of Milano. Since 1998 she is full time researcher at CNR-STIIMA, where she is currently responsible of the MEDIS research group, performing research activities in the field of micro engineering and robotics. She has been involved, with research and management role, in a variety of regional, national and European projects. She is member of the ASME/DAD Technical Committee on Micro Nano Systems. Since 2004 she is member of the executive board of SIRI (Italian Robotics and Automation Association). She is reviewer of international journals and conferences and author of more than 100 scientific papers of international journals, books and conference proceedings.

Luigi Tricarico. Full Professor from 2002 until today. His teaching and research activities concerns Manufacturing processes and Production systems. From the October 2009 until now is PhD coordinator of "Advanced Production Systems" - Polytechnic of Bari. Analysed topics are included in the following fields: Machining, Material Science and Technologies, Metal Forming processes, Non Traditional Manufacturing Processes, Computer Aided Manufacturing, CAD/CAM Integration. Actually, he coordinates and develops some research activities in Laser Material Processing, Metal Forming and Polymer Processing. Research results are shown in more than 200 papers published in national and international conferences proceedings and journals.